



AD-A282 905



**Evaluation of the Quality of Sapphire Using
X-ray Rocking Curves and Double-Crystal
X-ray Topography**

1 May 1994

Prepared by

P. M. ADAMS
Mechanics and Materials Technology Center
Technology Operations

Prepared for

SPACE AND MISSILE SYSTEMS CENTER
AIR FORCE MATERIEL COMMAND
2430 E. El Segundo Boulevard
Los Angeles Air Force Base, CA 90245

DTIC
ELECTE
AUG 02 1994
S G D

2308 **94-24293**

Engineering and Technology Group

 **THE AEROSPACE
CORPORATION**

APPROVED FOR PUBLIC RELEASE;
DISTRIBUTION UNLIMITED

DTIC QUALITY

94 8 01 050

This report was submitted by The Aerospace Corporation, El Segundo, CA 90245-4691, under Contract No. F04701-93-C-0094 with the Space and Missile Systems Center, 2430 E. El Segundo Blvd., Los Angeles Air Force Base, CA 90245. It was reviewed and approved for The Aerospace Corporation by S. Feuerstein, Principal Director, Mechanics and Materials Technology Center.

This report has been reviewed by the Public Affairs Office (PAS) and is releasable to the National Technical Information Service (NTIS). At NTIS, it will be available to the general public, including foreign nationals.

This technical report has been reviewed and is approved for publication. Publication of this report does not constitute Air Force approval of the report's findings or conclusions. It is published only for the exchange and stimulation of ideas.

Wm Kyle Sneddon, 13 May 94

Wm. Kyle Sneddon, Captain USAF
Deputy, Industrial & International Division
Plans and Programs Directorate
Phillips Laboratory

REPORT DOCUMENTATION PAGEForm Approved
OMB No. 0704-0188

Public reporting burden for this collection of information is estimated to average 1 hour per response, including the time for reviewing instructions, searching existing data sources, gathering and maintaining the data needed, and completing and reviewing the collection of information. Send comments regarding this burden estimate or any other aspect of this collection of information, including suggestions for reducing this burden to Washington Headquarters Services, Directorate for Information Operations and Reports, 1215 Jefferson Davis Highway, Suite 1204, Arlington, VA 22202-4302, and to the Office of Management and Budget, Paperwork Reduction Project (0704-0188), Washington, DC 20503.

1. AGENCY USE ONLY (Leave blank)		2. REPORT DATE 1 May 1994		3. REPORT TYPE AND DATES COVERED	
4. TITLE AND SUBTITLE Evaluation of the Quality of Sapphire Using X-ray Rocking Curves and Double-Crystal X-ray Topography				5. FUNDING NUMBERS F04701-93-C-0094	
6. AUTHOR(S) P. M. Adams					
7. PERFORMING ORGANIZATION NAME(S) AND ADDRESS(ES) The Aerospace Corporation Technology Operations El Segundo, CA 90245-4691				8. PERFORMING ORGANIZATION REPORT NUMBER TR-94(4935)-7	
9. SPONSORING/MONITORING AGENCY NAME(S) AND ADDRESS(ES) Space and Missile Systems Center Air Force Materiel Command 2430 E. El Segundo Boulevard Los Angeles Air Force Base, CA 90245				10. SPONSORING/MONITORING AGENCY REPORT NUMBER SMC-TR-94-32	
11. SUPPLEMENTARY NOTES					
12a. DISTRIBUTION/AVAILABILITY STATEMENT Approved for public release; distribution unlimited				12b. DISTRIBUTION CODE	
13. ABSTRACT (Maximum 200 words) Single-crystal sapphire is a material with a wide range of applications as a result of its unique physical, optical, mechanical, and chemical properties. The quality of a sapphire crystal can influence its effectiveness in many applications. High-quality, near-perfect, single-crystal sapphire can be grown, but it is difficult to shape and polish because of its extreme hardness, and surface flaws and damage are commonly produced during fabrication. Since this damage may exist in a buried subsurface layer, it can be difficult to detect. X-ray rocking curves and X-ray topography are extremely sensitive to the level of defects and strains in single crystals. A number of sapphire substrates, from several suppliers were examined using these techniques in order to determine how applicable they are for detecting defects in sapphire. A wide range in quality was found in sapphire received from different suppliers. Residual grinding/polishing damage was observed in many samples. Other defects observed included dislocations and mosaic structure and twinning in lower quality material. Rocking curves and double-crystal X-ray topography appear to be simple techniques for evaluating and determining the quality of sapphire. In particular, they are sensitive to subsurface damage and microscopic defects can be imaged at low to moderate magnification.					
14. SUBJECT TERMS Sapphire, X-ray diffraction, Crystal defects				15. NUMBER OF PAGES 20	
				16. PRICE CODE	
17. SECURITY CLASSIFICATION OF REPORT UNCLASSIFIED	18. SECURITY CLASSIFICATION OF THIS PAGE UNCLASSIFIED	19. SECURITY CLASSIFICATION OF ABSTRACT UNCLASSIFIED	20. LIMITATION OF ABSTRACT		

Preface

The author would like to thank J. Ciofalo, S. Gyetvay, J. Knudtson, and M. Tueling for providing sapphire samples for the study.

Accession For	
NTIS CRA&I	<input checked="checked" type="checkbox"/>
DTIC TAB	<input type="checkbox"/>
Unannounced	<input type="checkbox"/>
Justification	
By	
Distribution /	
Availability Codes	
Dist	Avail and/or Special
A-1	

Contents

1.	Introduction	1
2.	Experimental	3
3.	Results	5
3.1	(110) Orientation Sapphire	5
3.2	(001) Orientation Sapphire	9
3.3	(012) Orientation Sapphire	10
4.	Conclusions	15
	References	17

Figures

1. Schematic of double-crystal diffractometer.....	4
2. X-ray rocking curves from window quality (110) orientation sapphire substrates.....	5
3. (312) topographs of (110) orientation sapphire substrates with window polish surface finishes.....	7
4. (312) topographs of (110) orientation sapphire substrates with window polish surface finishes.....	8
5. X-ray rocking curves for window-grade and SOS-grade (001) sapphire substrates.....	9
6. (119) topographs of (001) orientation substrates.....	11
7. X-ray rocking curves from (012) orientation SOS and SOS-grade (without Si) sapphire.....	12
8. (223) reflection topographs of SOS-grade (012) orientation sapphire.....	14

Tables

1. Summary of Sapphire Samples Analyzed and Conditions for X-ray Rocking Curves and Double-Crystal X-ray Topography.....	2
---	---

1. Introduction

Single-crystal sapphire (α Al_2O_3) is a material that has found a wide range of applications as a result of its unique physical, optical, mechanical, and chemical properties. This material can provide ruby crystals for lasers; hard, high-strength, chemically resistant optical windows; and substrates for the growth of epitaxial films. The quality of a sapphire crystal can influence its effectiveness in many applications. In the case of substrates for epitaxial film growth, the quality and perfection of the epitaxial layer is often directly related to the quality of the underlying substrate. The strength of sapphire optical windows is also determined by the quality and level of defects. Even though high-quality, near-perfect, single-crystal sapphire can now be grown, it is difficult to shape and polish because of its extreme hardness. Surface flaws and defects, including twins,¹ are commonly produced during fabrication and may be difficult to detect or remove completely. These surface defects serve as crack initiation sites, which propagate and lead to premature failure when windows are stressed. Reference 2 provides an overview of methods used to remove surface defects from sapphire, thereby increasing its practical strength. Since many of these defects exist in a buried subsurface layer, they may be difficult to detect, and evaluating the effectiveness of surface treatments may be problematical.

X-ray rocking curves, which are recorded with a double-crystal diffractometer, are extremely sensitive to the level of defects and strains in single crystals. This extreme sensitivity and resolution is attained by using a nearly perfect crystal monochromator to produce an X-ray beam with very low divergence (<10 arc sec). The width of the rocking curve is an indication of the level of defects and/or deformation in the crystal. By flooding the sample with a very large X-ray beam and replacing the X-ray detector with a piece of film, it is possible to record an image (topograph) of the X-rays diffracted from the sample. Very minute defects can be easily imaged at relatively low magnification because ppm to ppb levels of strain, or lattice tilts of 1 arc sec in the crystal produce noticeable changes in X-ray intensity as a result of the very steep and narrow nature of the rocking curve. That is, very microscopic defects have macroscopic deformation fields (at the ppm level) associated with them and can easily be seen in the X-ray topographs. Since X-rays penetrate several to tens of microns into a material, rocking curves and X-ray topographs can be used to obtain information on buried damaged layers produced by grinding and polishing. Examples of the types of defects that can be imaged in the topographs include local lattice curvature, mosaic structure, individual dislocations, and residual polishing/grinding damage. Low-resolution images of highly perfect crystals can be recorded rather quickly (10–15 min), while high-resolution images require much longer ($\times 10$) time because of the very slow speed of the high-resolution film.

Sapphire has been studied in the past^{3–13} by other X-ray topographic techniques, but these methods do not have the strain sensitivity of the double-crystal diffractometer. Single-crystal sapphire may be grown by a variety of different methods, of which the more common are Verneuil (flame fusion), Czochralski, flux, and hydrothermal.³ The types and number of defects associated with each method of growth may vary.^{3–5} Most commercially available sapphire is grown by either the Verneuil or Czochralski techniques. The Czochralski method, under the

proper conditions, can produce very large (> 3 in. diam) crystals with relatively low defect concentrations.

A number of sapphire substrates, from several suppliers and of potentially different quality, were examined using X-ray rocking curves and double-crystal X-ray topography (DCXT) in order to determine how applicable the techniques are for evaluating the quality of sapphire. Table 1 summarizes the commercially available sapphire samples analyzed using X-ray rocking curves and DCXT. The sapphire crystals studied were of different grades, had three different crystallographic orientations, and were from two different suppliers. The orientations of the samples along with the X-ray reflections used for rocking curves and DCXT are also given in Table 1. The samples had different surface finishes, ranging from window to epitaxial polishes. The latter finish is used on some silicon-on-sapphire (SOS) grade material and uses a "Syton" (colloidal silicon with NaOH) final polish to remove coarser polishing damage. One sample of window-grade material was etched with molten KHSO_4^5 to remove surface defects before the rocking curve/DCXT analyses; all other samples were analyzed as received.

Table 1. Summary of Sapphire Samples Analyzed and Conditions for X-ray Rocking Curves and Double-Crystal X-ray Topography

Sample/Orientation	Comments	Reflections Used for Rocking Curves	Reflections Used for Topographs
A. Moller/(001) ⁺	Window Grade	(00 12)	
		(119)	(119)
Union Carbide/(001)	SOS Grade	(00 12)	
	(No Silicon)	(119)	(119)
OTF [#] /(110)	Poor Quality	(220)	
	Unetched	(312)	(312)
OTF(A)/(110)	Good Quality		
	Unetched	(312)	(312)
OTF/(110)	Etched with	(220)	
	KHSO ₄	(312)	(312)
SOS/012)	Silicon on	(024)	
	Sapphire (SOS)	(223)	(223)
OTF Side 1/(012) [*]	SOS Grade	(024)	
	(No Silicon)	(223)	(223)
	Epitaxial Polish		
OTF Side 2/(012) [*]	SOS Grade	(024)	
	(No Silicon)	(223)	(223)
	Window Polish		

+ = Abbreviated notation: (hkl). [in hexagonal system for (hkil); i = -(h+k)]

* = Different sides of same sample

= OTF Supplier not specified

2. Experimental

A commercially available (Blake Industries) double-crystal diffractometer equipped with a copper X-ray tube was used in the rocking curve and DXRT analyses. Two configurations in the (+, -) unequiaspacing mode were used to obtain rocking curves; the schematics are given in Figure 1. In the first case (Figure 1a), a $\langle 100 \rangle$ Ge monochromator was set for diffraction from the (400) reflection, and a slit was used to monochromatize ($K_{\alpha 1}$) the diffracted beam and limit its size to approximately $0.5 \text{ mm} \times 0.5 \text{ mm}$. This monochromatic X-ray beam was then diffracted from a set of crystallographic planes parallel to the surface of the sapphire substrate. For example, with a (001) orientation sapphire substrate a (00 12) reflection was used. The sample was aligned by tilting about a horizontal axis and "rocking" about a vertical axis while the intensity was monitored with a scintillation detector. The sample was also translated during the alignment as a check on uniformity. The sample was aligned for maximum intensity and then "rocked" with a scan speed of 50 arc sec/minute using a dc continuous motor. Rocking curves were recorded with a computer by collecting the diffracted intensity with a short time constant (0.1 s).

Rocking curves were also obtained in a second configuration (Figure 1b) in preparation for the recording of DXRT images. In these cases, the $\langle 100 \rangle$ Ge monochromator was aligned for diffraction from the (422) reflection so that the X-ray beam would be expanded, and the area illuminated on the sample crystal maximized. Slits were used to monochromatize ($K_{\alpha 1}$) the diffracted beam, and its size was limited to approximately $3\text{--}4 \text{ mm} \times 25 \text{ mm}$. Depending on the crystallographic orientation of the sapphire substrate, a reflection was selected such that the X-ray beam was incident on the sample at a small angle ($<10^\circ$) and that the angle (2θ) between the incident and diffracted beam was approximately 90° . In most cases, this resulted in an area of the sample of about $10 \text{ mm} \times 25 \text{ mm}$ being illuminated. The samples were aligned to provide the maximum diffracted intensity at a single angular position. An image intensifier, which allowed real-time visualization of the diffracted X-ray beam, was also helpful in the alignment. Rocking curves were recorded at a scan speed of 500 arc sec/min. The topographic images were obtained with the sample stationary and positioned at the maximum intensity of the rocking curve. Topograph images were recorded with Ilford L-4 Nuclear emulsion film.

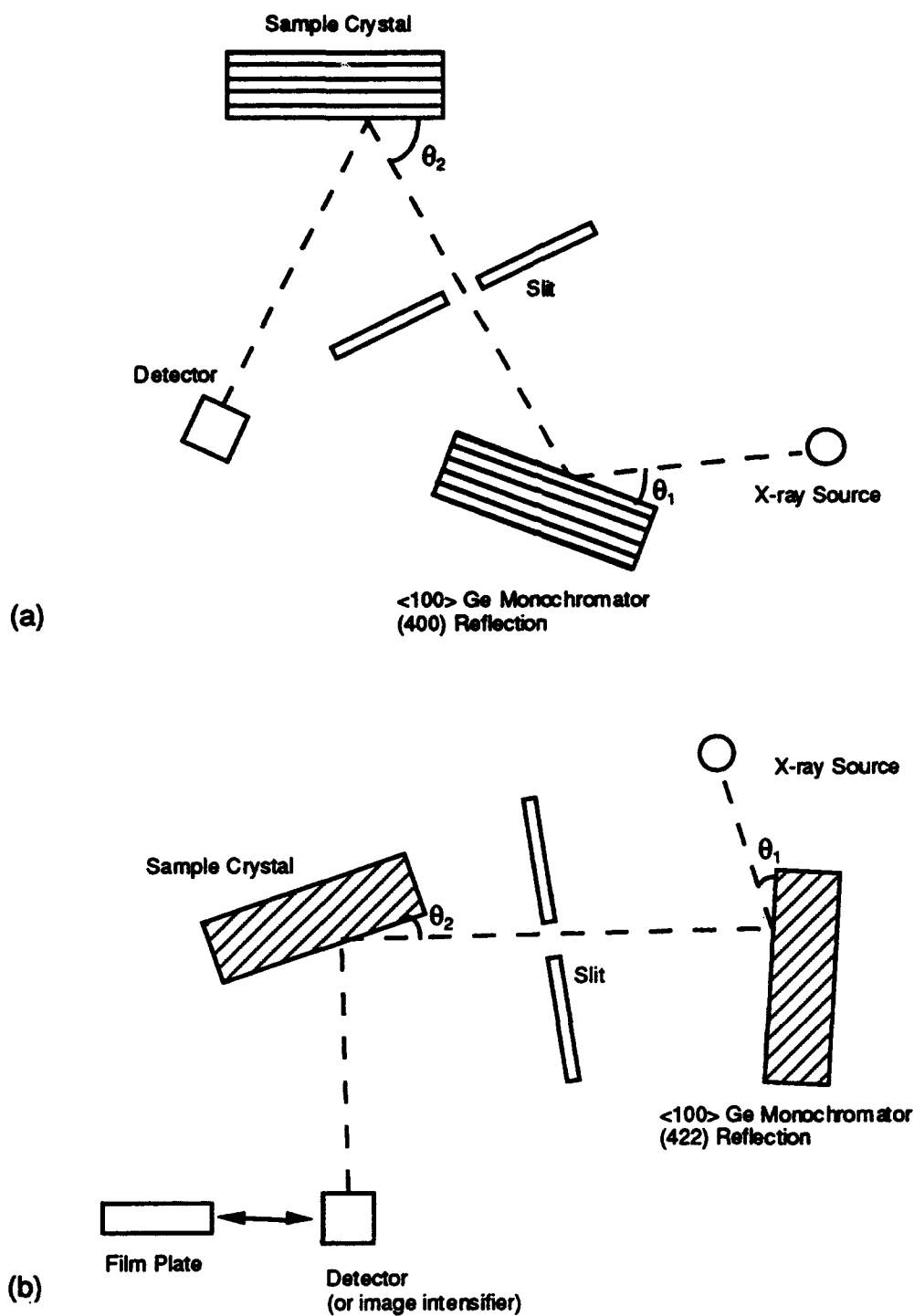


Figure 1. Schematic of double-crystal diffractometer. (a) set for obtaining rocking curves from lattice planes parallel with the sample surface ($\theta_1 = 33^\circ \neq \theta_2$); (b) aligned for reflection topography. Detector is used to obtain rocking curve. Topograph is recorded by film with sample positioned at maximum intensity of rocking curve. [$\theta_1 = 7^\circ \neq \theta_2$ (typically $<10^\circ$)].

3. Results

3.1 (110) Orientation Sapphire

Four (110) orientation sapphire substrates supplied by Adolf Meller Co. were examined with a combination of X-ray rocking curves and double-crystal X-ray topographs. The grade of the substrates was unspecified, and it is assumed that they had window finishes on both sides. Figure 2a shows the (220) rocking curves with the highest intensity and narrowest full widths at half maximum (FWHM) obtained from areas (0.5×0.5 mm) on two different substrates—one as-received and the other after being etched with molten KHSO_4 to remove surface defects. The rocking curve of the as-polished surface is relatively broad and non-Gaussian in shape and has a FWHM of 56 arc sec. In comparison, the (220) rocking curve of the etched sample is much narrower (28 arc sec) and symmetric in shape, indicating that the surface is more defect free,

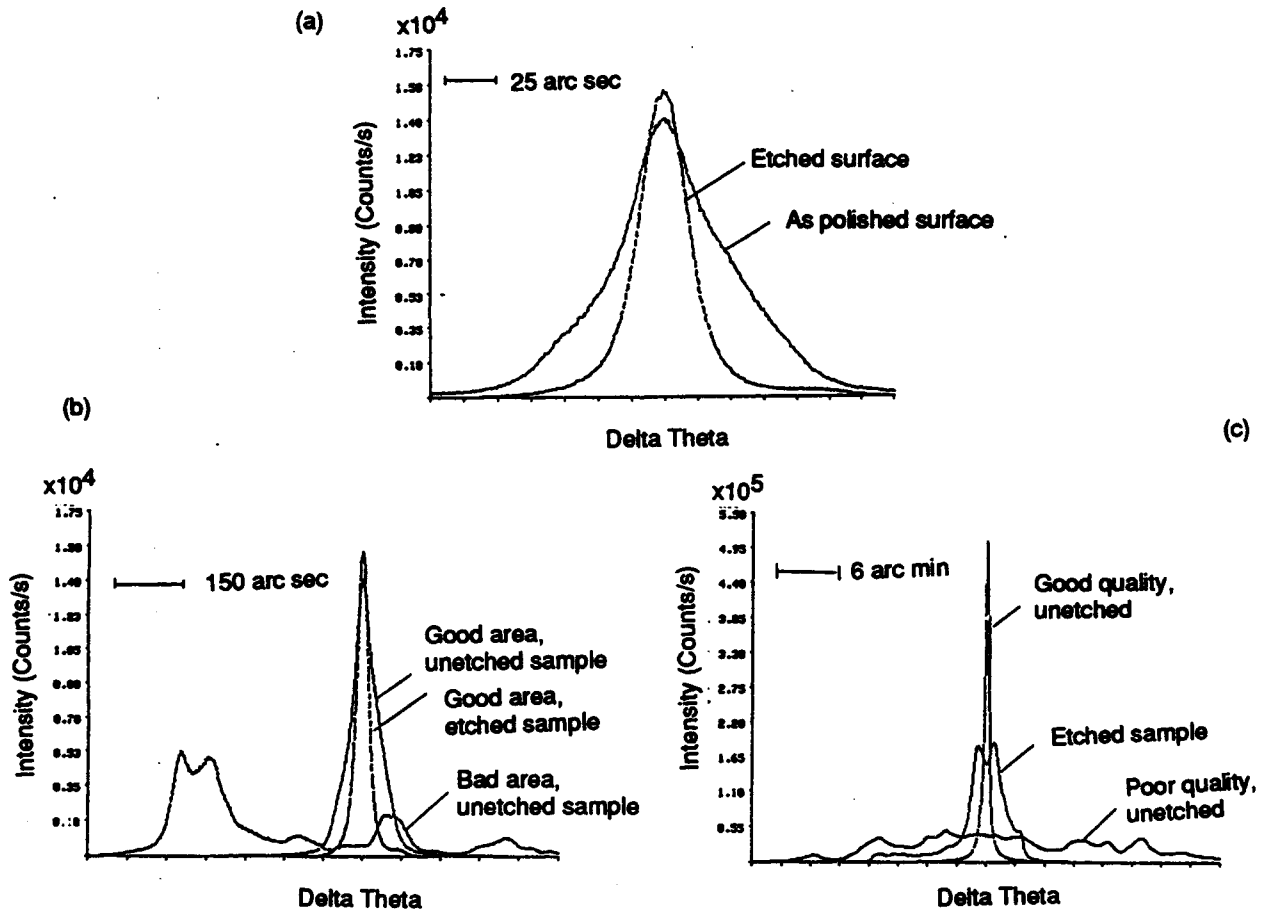


Figure 2. X-ray rocking curves from window quality (110) orientation sapphire substrates: (a,b) (220) reflections of small selected areas ($0.5 \text{ mm} \times 0.5 \text{ mm}$); (c) (312) reflections of large areas ($10 \text{ mm} \times 25 \text{ mm}$) before topographs.

although visually it has a frosted appearance. It is noted that the rocking curves of the two samples varied greatly with position, and Figure 2b shows the rocking curve from a poorer area of the unetched sample compared with the plots in Figure 2d. It exhibits multiple broad peaks, indicative of angular misorientations within the sample, either as a result of mosaic structures (low-angle boundaries) or lattice distortion (warpage).

The (312) rocking curves of these two samples, plus that of a third unetched specimen (with 300 nm SiO_2 + 300 nm Al_2O_3 amorphous film), were recorded prior to taking double-crystal topographs and are given in Figure 2c. The corresponding (312) topographs are presented in Figures 3a, 3b, and 4a. The (312) topograph of a fourth sample, for which rocking curves were not recorded, is given in Figure 4b. From the rocking curves, it can be seen that a wide variation in quality exists between samples obtained from the same supplier and that lattice misorientations can vary from 0.5 to 40 arc min between samples. Several features are visible in the topographs of the unetched sample in Figure 3a. The majority of the sample is not imaged, indicating a high degree of warpage in the crystal lattice. The dark irregular pattern represents only that portion of the sample that is suitably oriented for diffraction (Bragg angle contour). All other areas are angularly misoriented. Also visible are some relatively straight demarcations (S in Figure 3a), which probably represent subgrain boundaries across which there is an abrupt, slight orientation change. Scratch-like features are conspicuous in the topograph and represent surface scratches or subsurface residual polishing damage. These are visible in many areas of the topographs, which otherwise are not diffracting, because strains from the damage put areas around the damage into a diffracting orientation/condition. Linear features (L), which may represent slight variations in lattice parameter along the crystal growth front, or dislocation networks, and small inclusions (I) or voids, are also visible in the topograph.

For comparison, the topograph of the etched sample is given in Figure 3b. It also displays a high degree of lattice warpage and some linear features, which may be subgrain boundaries, but the scratch-like polishing damage is no longer visible. This indicates that the etch was successful in removing the surface damage. The topograph of the sample, which produced a very narrow (312) rocking curve (Figure 2c), is given in Figure 4a. Residual polishing damage is still prominent; however, a much larger area of this sample is in a diffracting condition, indicating that there is less angular misorientation (warpage) within the sample. The margins of the amorphous film (F) are also visible in the topograph.

A topograph of a fourth substrate, for which a rocking curve was not recorded, is given in Figure 4b. It also displays a high degree of lattice warpage and many linear boundaries that may represent subgrain or twin boundaries. Based on the topographs of these four (110) orientation sapphire substrates, it can be seen that a wide range of quality exists and that the type of damage/defects also differ dramatically. This may result from substrates being cut from crystals grown by different methods (Verneuil vs. Czochralski) or varying in quality, and/or quality varying within any given crystal.⁴

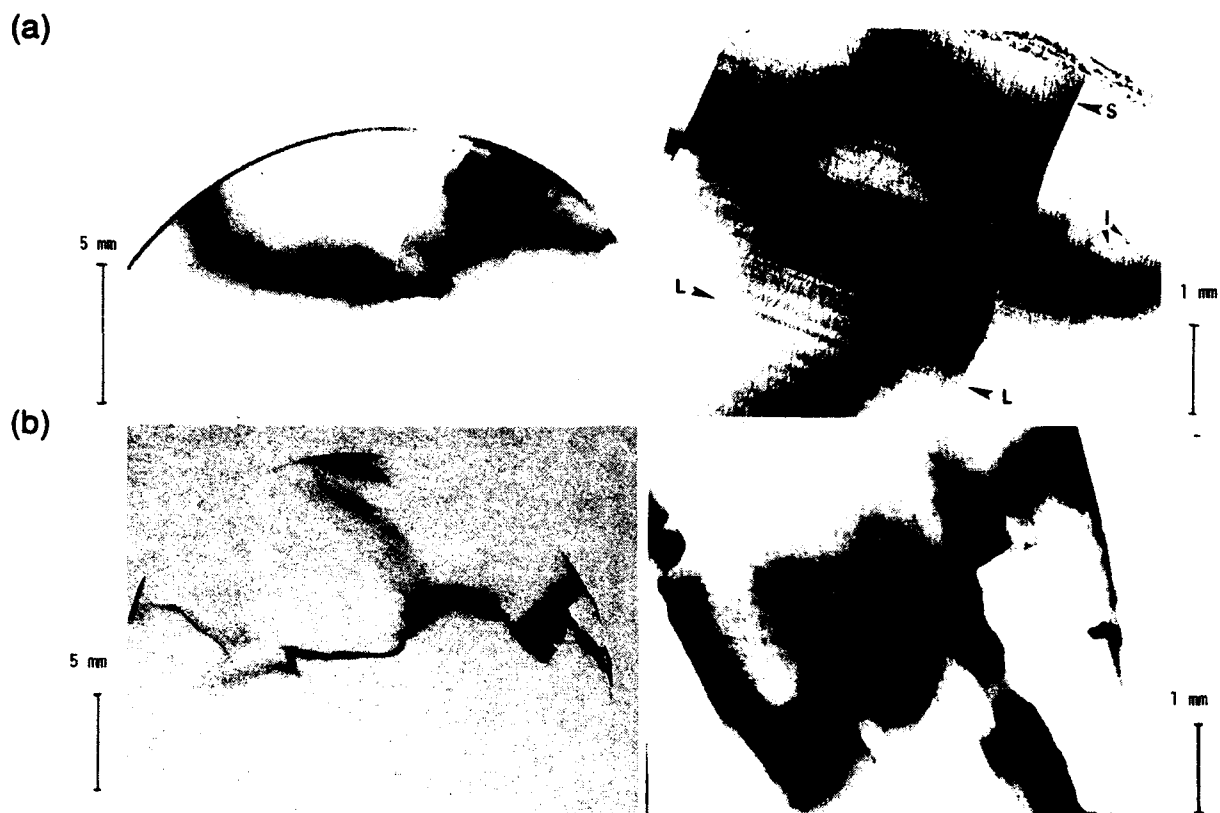


Figure 3. (312) topographs of (110) orientation sapphire substrates with window polish surface finishes. (a) as-received; (b) after etching to remove surface defects.

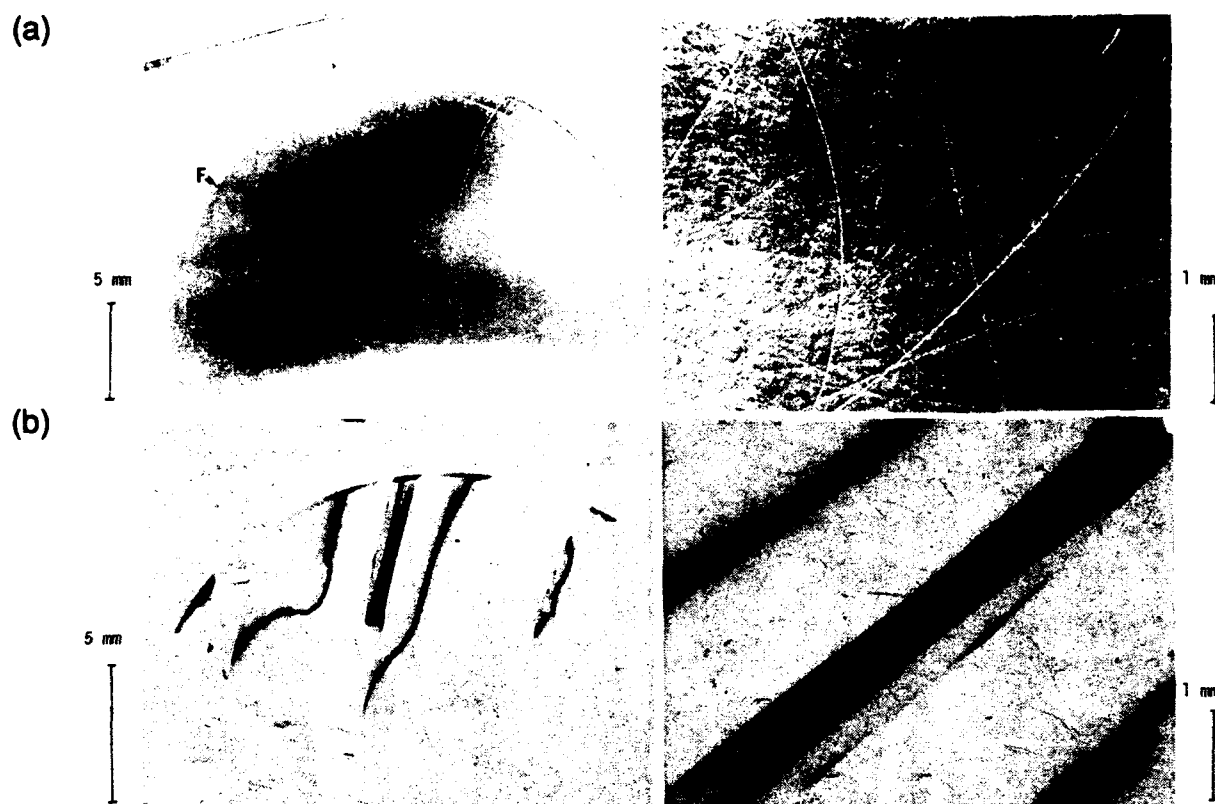


Figure 4. (312) topographs of (110) orientation sapphire substrated with window polish surface finishes. (a) good quality substrate with amorphous film (F); (b) poor quality substrate.

3.2 (001) Orientation Sapphire

Two samples of (001) orientation sapphire were examined by X-ray rocking curves and DXRT. One sample was of window-grade material obtained from Adolf Meller Co., while the other was SOS grade (without silicon epitaxial layer) purchased from Union Carbide. The (00 12) rocking curves of both samples are given in Figure 5a; they are approximately equivalent in intensity and FWHM (26–28 arc sec). In comparison, the (119) rocking curves obtained prior to taking topographs are shown in Figure 5b. The SOS grade sample exhibits a very narrow (FWHM ~ 50 arc sec) single peak, whereas the window-grade material displays extended multiple peaks over an

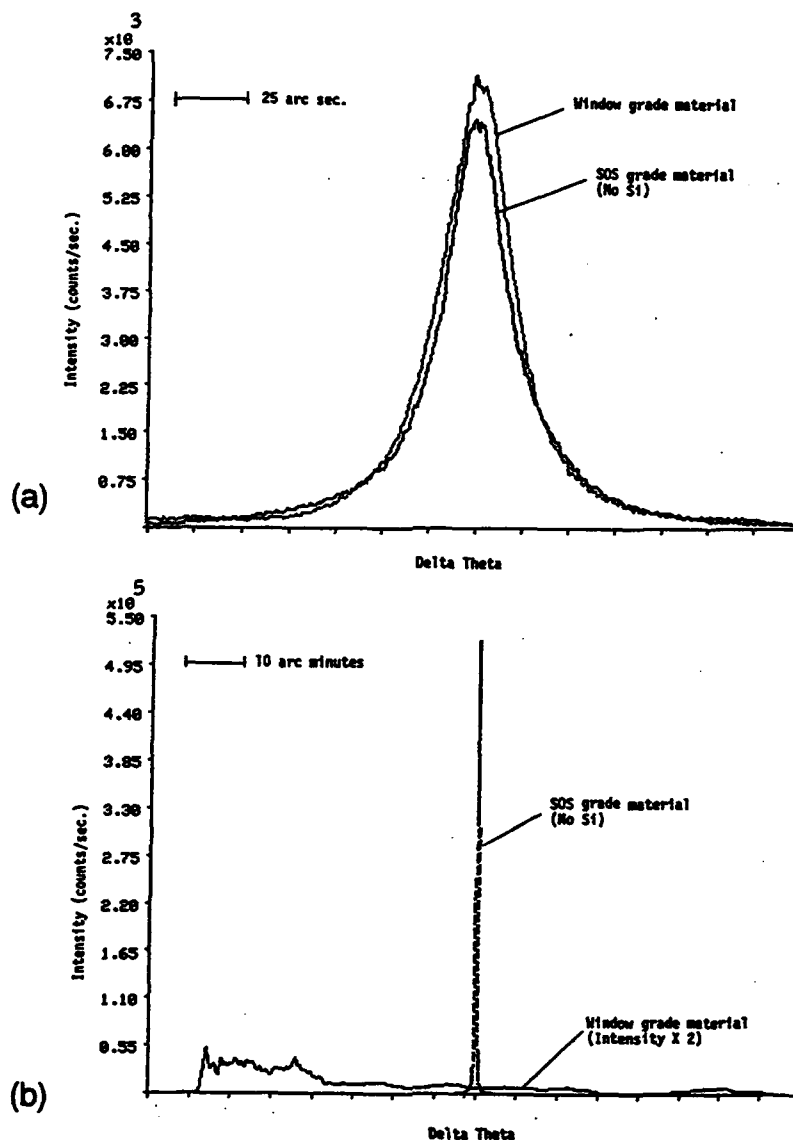


Figure 5. X-ray rocking curves for window-grade and SOS-grade (001) sapphire substrates. (a) (00 12) reflections of selected areas (0.5 mm \times 0.5 mm); (b) (119) reflections of large areas (10 mm \times 25 mm) before topograph.

angular range of more than $1.5^\circ \Delta\theta$. This indicates large lattice distortions and/or low-angle boundaries, with misorientation in excess of 1.5° within the window-grade sample. The difference in the (119) rocking curves of both samples, in comparison to the (00 12) rocking curves, is attributed to the former having a much larger area of analysis. On the small scale ($0.5 \text{ mm} \times 0.5 \text{ mm}$) of the (00 12) rocking curves, both samples appear to have some areas of comparable quality. On the large-scale ($10 \text{ mm} \times 25 \text{ mm}$) coverage of the (119) rocking curves, however, the SOS grade sample has a very high degree of lattice orientation uniformity, whereas the window grade material is very imperfect.

The (119) topographs of the two (001) samples are given in Figure 6. The topograph (Figure 6a) of the SOS-grade material shows a large area diffracting uniformly. Superimposed on this are frequent dislocations (D) and subtle linear (L) contrast variations, which may reflect slight variations in lattice parameter. Basal dislocations have been previously reported for sapphire.^{8,9} Topographs were taken on three positions of the rocking curve of the window-grade sample because of the low intensities and extended angular range. The three (A-C) superimposed images are given in Figure 6b. Very irregularly shaped areas are diffracting at any one position on the rocking curve, and these are separated by large areas that are completely out of the diffracting condition. This is consistent with the large lattice misorientations and warpage indicated in the rocking curves. The almost helical-appearing images (C) are particularly interesting. Helical dislocations have been observed⁹ as a result of dislocation interaction during annealing, but these are usually much smaller ($100\text{--}500 \mu\text{m}$) in size. The observed features may be large helical dislocation networks, but this has not been confirmed since the overall poor quality of the material does not make it suitable for its intended application.

3.3 (012) Orientation Sapphire

Two samples of silicon-on-sapphire (SOS) grade (012) orientation sapphire obtained from Union Carbide were examined with X-ray rocking curves and DCXT. One sample was true SOS and had a $0.6 \mu\text{m}$ epitaxial layer of silicon on the sapphire. The sapphire substrate was studied through the silicon epitaxial layer since it did not appreciably attenuate the X-ray beam and because the back surface had not been polished. The other sample was SOS-grade sapphire without a silicon epitaxial layer. Both sides of this sample were examined since they differed in surface finish. One supposedly had received an epitaxial ("Syton") polish and the other a window polish.

The (024) rocking curves of these samples are given in Figure 7a. The intensity of the SOS sample is the lowest since its surface was covered with the silicon epitaxial layer. Otherwise, the three rocking curves are similar in quality ($\text{FWHM} = 17\text{--}20 \text{ arc sec}$), although the intensity of the side with the epitaxial polish is slightly higher. The (223) rocking curves of the SOS-grade sapphire samples obtained before DXRT are given in Figure 7b. Even though large areas ($10 \text{ mm} \times 25 \text{ mm}$) of the sample were covered in the analyses, the rocking curves are very narrow ($\text{FWHM} = 22\text{--}56 \text{ arc sec}$). This indicates a high degree of uniformity in the lattice, with very little distortion and low levels of defects. The two rocking curves from the sample lacking a silicon epi-layer cannot be compared due to the very high count rates ($> 5 \times 10^5 \text{ cps}$). At these levels, the detector becomes affected by dead time in response to the X-rays, and it becomes difficult to get an accurate measure of the intensity. This makes alignment of the sample for maximum intensity difficult and causes the rocking curves to have distorted shapes ("clipped tops").



Figure 6. (119) topographs of (001) orientation substrates. (a) SOS-grade material (without Si); note dislocations (D); (b) window-grade material.

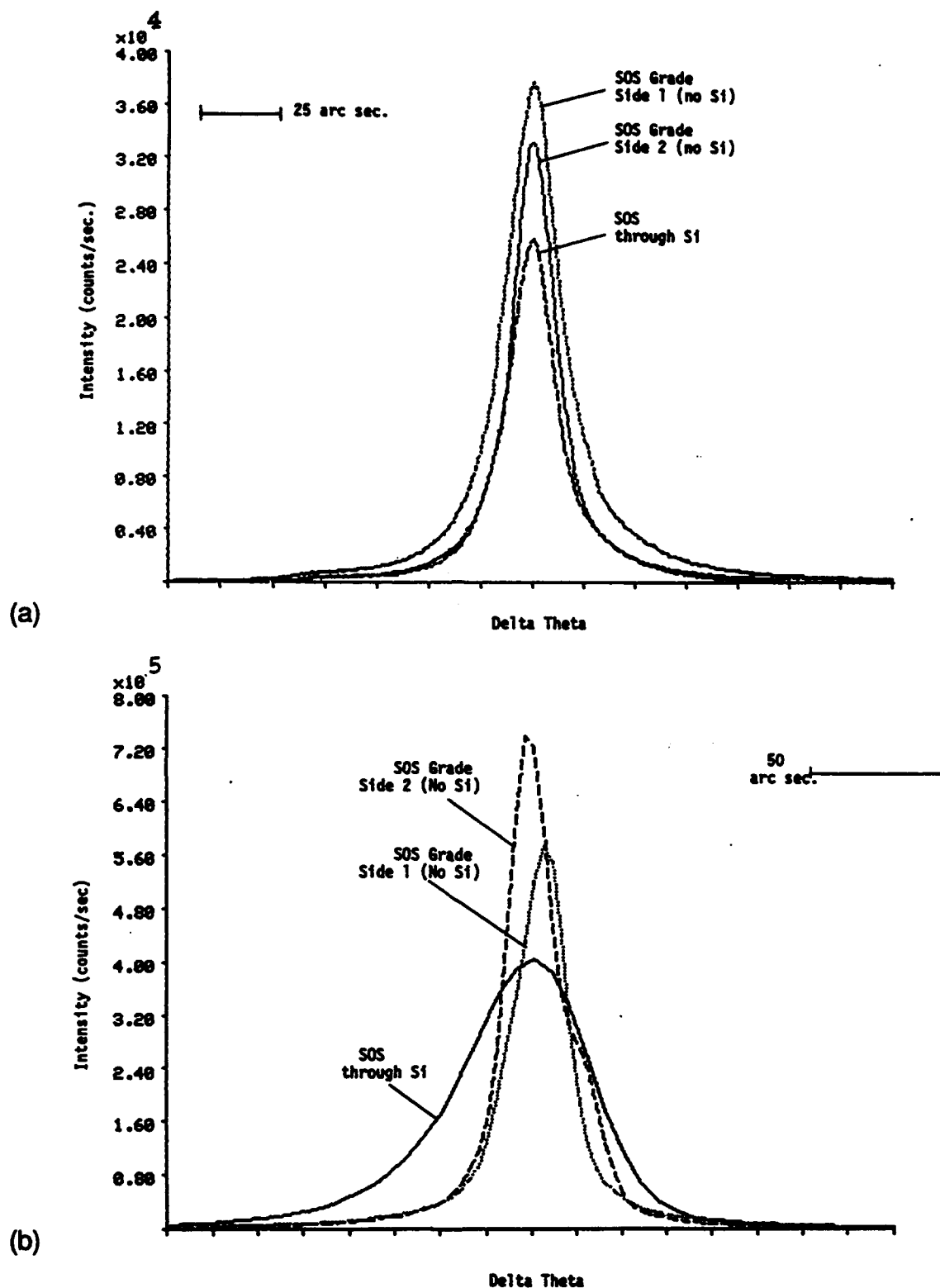


Figure 7. X-ray rocking curves from (012) orientation SOS and SOS-grade (without Si) sapphire. (a) (024) reflections of small selected areas (0.5 mm x 0.5 mm); (b) (223) reflections of large areas (10 mm x 25 mm) before topographs.

The (223) topographs of these samples are given in Figure 8. The topograph of the SOS sample, shown in Figure 8a, shows a large area of coverage and fine-scale defect structures. These defects are interpreted as dislocations, but unlike those visible in the (001) orientation SOS-grade sapphire, they appear as very short segments since they are being viewed in cross section. The topographs of the two sides of the sample lacking the silicon epi-layer are given in Figures 8b and c. The side shown in Figure 8b was supposed to have a window finish and was marked by two fiducial marks (scratches). Several scratches or residual polishing damage are visible in addition to dislocation-like features. The opposite side of the sample was supposed to have an epitaxial finish, but even more residual polishing damage is visible in the topograph (Figure 8c), along with dislocation-like structures. Both sides of the samples show large areas of coverage in the topographs. Based on the DXRT analyses, it can be seen that even some sapphire surfaces, which are supposed to have an epitaxial finish, may have residual polishing damage. Furthermore, based on the amount of observed damage on this one specimen, it is uncertain whether the fiducial marks were placed on the correct side of the sample since less damage was seen on the side designated as having the window polish. For comparison, the topograph of the (001) orientation SOS-grade sapphire (Figure 6a) and true SOS (Figure 8a) show no signs of residual polishing damage. In the case of the (001) sample, the surface finish was unspecified, and it was assumed it received a window polish.

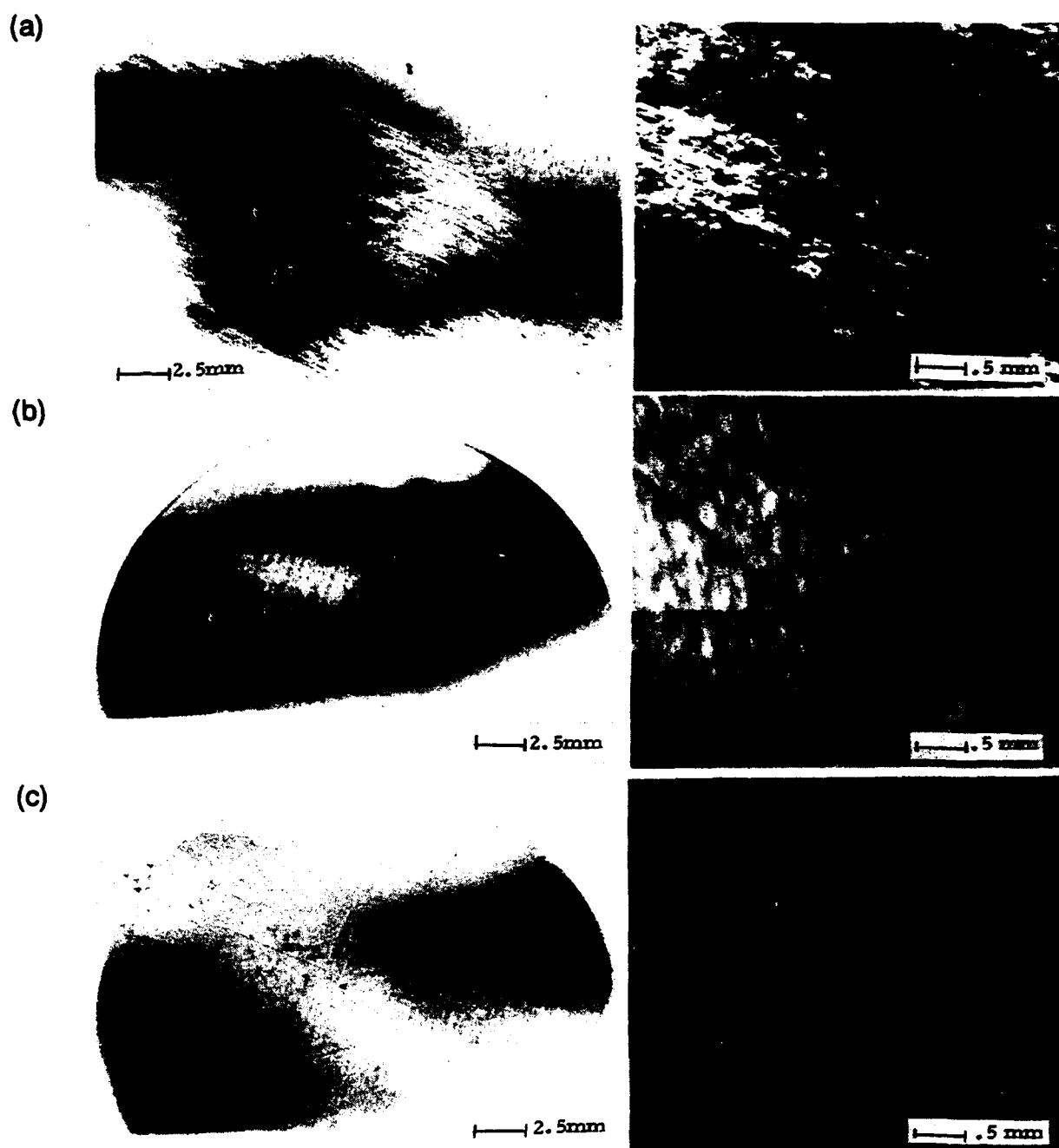


Figure 8. (223) reflection topographs of SOS-grade (012) orientation sapphire. (a) SOS; topograph taken through 0.6 μm of silicon. (b,c) sides 1 and 2 of SOS-grade sapphire without silicon epitaxial layer.

4. Conclusions

It can be seen from the X-ray rocking curve and double-crystal topographic analyses that a wide range in quality exists in single-crystal sapphire received from different suppliers, and even from an individual supplier. Overall, the material obtained from Union Carbide (SOS grade) appeared to be superior, but some variations in quality were still observed.

Residual grinding/polishing damage was observed in many samples, including some that were reported to have an epitaxial finish. Other defects observed included dislocations, and mosaic structure and twinning in lower quality material. Based on the limited number of samples studied and the wide variation in quality observed, it seems prudent that some form of verification of quality be performed upon receipt of samples if the highest quality material is required. Since visual inspection is inadequate, rocking curves and double-crystal X-ray topography appear to be simple techniques for evaluating and determining if samples meet specifications and expectations. In particular, they are sensitive to subsurface damage and microscopic defects can be imaged at low to moderate magnification.

References

1. P. F. Becher, "Abrasive surface deformation of sapphire," *J. Amer. Ceram. Soc.*, **59**, 143–154, (1976).
2. S. C. Bates and L. Liou, "High Performance Sapphire Windows," NASA Conference Pub. 3189, **2**, 460–469, (1992).
3. R. Belt, "Lang X-ray Topographic Studies of Ruby Grown by Different Methods," *Adv. X-ray Analysis* (Plenum), **10**, p. 159–172 (1967).
4. V. Yip, and C. Brandle, "Low-Angle Grain Boundary Macrostructure in Large Diameter Czochevski white sapphire," *J. Am. Ceram. Soc.* **61**, p. 8–13, (1978).
5. K. Janowski, A. Chase, and E. Stofel, "Growth Defects in Flux-Grown Rubies," *Trans. Metall. Soc. AIME*, **233**, p. 2087–2091, (1965).
6. Y. Takano and K. Kohn, "X-ray Studies of Dislocation Structures in a Sapphire Crystal," *Japan J. Appl. Phys.*, **9**, p. 847–848, (1970).
7. C. May, and J. Shah, "Dislocation Reactions and Cavitation Studies of Melt Grown Sapphire," *J. Mater. Sci.*, **4**, 179–188, (1969).
8. J. Caslavsky, C. Gazzara, and R. Middleton, "The Study of Basal Dislocations in Sapphire," *Phil. Mag.*, **25**, p. 35–44, (1971).
9. J. Caslavsky and C. Gazzara, "Dislocation Behavior in Sapphire Single Crystals," *Phil. Mag.*, **26**, p. 961–975, (1972).
10. L. Birks, J. Hurley, and W. Sweeney, "Perfection of Ruby Laser Crystals," *J. Appl. Phys.*, **36**, p. 3562–3565, (1965).
11. Z. Qiang, D. Peizhen, and G. Faxi, "X-ray topographic investigation of characteristic dislocation structure in sapphire single crystals," *J. Appl. Phys.*, **67**, 6159–6164, (1990).
12. K. Wada and K. Hoshikawa, "Growth and characterization of sapphire ribbon crystals," *J. Crystal Growth*, **50**, 151–159, (1980).
13. E. N. Farabaugh, H. S. Parker, and R. W. Armstrong, "Skew-reflection X-ray microscopy of the vapor-growth surface of an Al_2O_3 single crystal," *J. Appl. Cryst.*, **6**, 482–486, (1973).

TECHNOLOGY OPERATIONS

The Aerospace Corporation functions as an "architect-engineer" for national security programs, specializing in advanced military space systems. The Corporation's Technology Operations supports the effective and timely development and operation of national security systems through scientific research and the application of advanced technology. Vital to the success of the Corporation is the technical staff's wide-ranging expertise and its ability to stay abreast of new technological developments and program support issues associated with rapidly evolving space systems. Contributing capabilities are provided by these individual Technology Centers:

Electronics Technology Center: Microelectronics, solid-state device physics, VLSI reliability, compound semiconductors, radiation hardening, data storage technologies, infrared detector devices and testing; electro-optics, quantum electronics, solid-state lasers, optical propagation and communications; cw and pulsed chemical laser development, optical resonators, beam control, atmospheric propagation, and laser effects and countermeasures; atomic frequency standards, applied laser spectroscopy, laser chemistry, laser optoelectronics, phase conjugation and coherent imaging, solar cell physics, battery electrochemistry, battery testing and evaluation.

Mechanics and Materials Technology Center: Evaluation and characterization of new materials: metals, alloys, ceramics, polymers and their composites, and new forms of carbon; development and analysis of thin films and deposition techniques; nondestructive evaluation, component failure analysis and reliability; fracture mechanics and stress corrosion; development and evaluation of hardened components; analysis and evaluation of materials at cryogenic and elevated temperatures; launch vehicle and reentry fluid mechanics, heat transfer and flight dynamics; chemical and electric propulsion; spacecraft structural mechanics, spacecraft survivability and vulnerability assessment; contamination, thermal and structural control; high temperature thermomechanics, gas kinetics and radiation; lubrication and surface phenomena.

Space and Environment Technology Center: Magnetospheric, auroral and cosmic ray physics, wave-particle interactions, magnetospheric plasma waves; atmospheric and ionospheric physics, density and composition of the upper atmosphere, remote sensing using atmospheric radiation; solar physics, infrared astronomy, infrared signature analysis; effects of solar activity, magnetic storms and nuclear explosions on the earth's atmosphere, ionosphere and magnetosphere; effects of electromagnetic and particulate radiations on space systems; space instrumentation; propellant chemistry, chemical dynamics, environmental chemistry, trace detection; atmospheric chemical reactions, atmospheric optics, light scattering, state-specific chemical reactions and radiative signatures of missile plumes, and sensor out-of-field-of-view rejection.



2350 E. El Segundo Boulevard
El Segundo, California 90245-4691
U.S.A.